SPAWAR
Systems Center
PACIFIC

TECHNICAL REPORT 2049
September 2014

Investigation of the Effects of Oxygen Content in $YBa_2Cu_3O_x$ on the Depth and Profile of Direct Ion Trenches

Benjamin Taylor
Teresa Emery
Susan Berggren

SSC Pacific
San Diego, CA 92152-5001

TECHNICAL REPORT 2049
September 2014

Investigation of the Effects of Oxygen Content in $YBa_2Cu_3O_x$ on the Depth and Profile of Direct Ion Trenches

Benjamin Taylor
Teresa Emery
Susan Berggren

SSC Pacific
San Diego, CA 92152-5001

SSC Pacific
San Diego, California 92152-5001

K. J. Rothenhaus, CAPT, USN
Commanding Officer

C. A. Keeney
Executive Director

ADMINISTRATIVE INFORMATION

The work described in this report was performed by the Advanced Analysis Systems Branch (Code 71730) of the ISR Division (Code 71700), Space and Naval Warfare Systems Center Pacific (SSC Pacific), San Diego, CA. The Naval Innovative Science and Engineering (NISE) Program at SSC Pacific funded this Applied Research project.

.

Released by
K. S. Simonsen, Head
Advanced Analysis Branch

Under authority of
A. D. Ramirez, Head
ISR Division

SB

EXECUTIVE SUMMARY

OBJECTIVE

Research being carried out in the Cryogenic Exploitation of Radio Frequency (CERF) laboratory at Space and Naval Warfare Systems Center Pacific (SSC Pacific) into the development of advanced superconducting RF sensors known as Superconducting Quantum Interference Device (SQUID) arrays is transitioning from the development and study of devices fabricated from the low-temperature superconductor niobium to system deployable devices made from the high-temperature superconductor $YBa_2Cu_3O_{7-\delta}$. A research effort began in FY12 under the SSC Pacific Naval Innovative Science and Engineering (NISE) Program in advance of this transition to investigate relevant fundamental electronic properties of the compound $YBa_2Cu_3O_x$ ($6 \leq x \leq 7$). A significant result from the NISE project involved the invention of a novel method and subsequent development of an apparatus by which a single film could be grown with a monotonically varying oxygen content as a function of the physical distance along the sample, which we refer to as $YBa_2Cu_3O_{\bigtriangledown x}$. The purpose of this approach is to enable an examination of the evolution of the electronic tunneling properties as a function of oxygen content in a nearly continuous fashion, thereby providing an experimental resolution previously unobtainable. Josephson junctions can be fabricated via many known methods; however, a particularly useful method for our purposes involves the use of a directed ion beam to disorder or mill away a region of the film. Because the ion milling process is material dependent it becomes necessary to establish whether, and to what extent, the level of oxygen affects the resulting junction formation geometry. The objective of this study is to systematically investigate and determine the impact of local oxygen content on the ion milling profile on a film of $YBa_2Cu_3O_{\bigtriangledown x}$. Presented here are the preliminary results from this study.

RESULTS

Based on initial experiments and measurements, we find a significant correlation of local oxygen content on the depth and profile of micro-meter scale trenches ion milled on the surface of the $YBa_2Cu_3O_{\bigtriangledown x}$ film. An identical configuration of the ion milling apparatus were used on all exposed areas, thereby leaving oxygen content as the only experimental variable. A brief analysis suggests that oxygen ordering is responsible for the change in milling results within the range of oxygen levels examined.

RECOMMENDATIONS

Further measurements and analysis are underway. Currently, it appears that the change in the ion milling profile can be used advantageously in the fabrication of Josephson junction on films of $YBa_2Cu_3O_{7-\delta}$, wherein the film is annealed such that the oxygen content of the sample is set to an ideal level for a controlled profile result, and then re-annealed for desired electronic properties. Alternatively, if a device is to be made from a non-uniform $YBa_2Cu_3O_{\bigtriangledown x}$ film, then the configuration of the ion milling apparatus will need to be modified accordingly depending upon the local oxygen content of the region to be milled.

CONTENTS

EXECUTIVE SUMMARY ..... **iii**

1. INTRODUCTION **1**

2. EXPERIMENT **3**

3. RESULTS & ANALYSIS **5**

4. CONCLUSION **7**

REFERENCES **7**

Figures

1. (a) 2-D profile taken from a section of the 3-D AFM images of ion milled trenches taken at locations having the CuO_2 plane doping values indicated. An upper limit on the error of the p values is estimated as Δp = 0.002. (b) 3-D AFM image of the ion milled trench taken at $p \approx 0.121$. (c) 3-D AFM image of the ion milled trenche taken at $p \approx 0.125$. 4

2. (a) Lattice structure of fully oxygenated $YBa_2Cu_3O_7$. Cu-O chains are highlighted with blue dashed ovals. The superconducting CuO_2 planes are highlighted with red dashed panels. For clarity, not all oxygen atoms are shown in the CuO_2 plane. (b) Oxygen ordering in the plane containing the Cu-O chains. Depicted are the well-ordered chain states with $x = 7.0$ ($p \approx 0.20$) and $1/8^{th}$ doping ($x \approx 6.71$) states, as well as the disordered (broken chain) state with $p \lesssim 1/8$. (c) Depiction of the direct ion milling process used to fabricate Josephson junctions in $YBa_2Cu_3O_{7-\delta}$ along with the resulting trench profile in the two regions having doping values indicated in panel (b) above. As described in the main text, Ga^+ ions impact the uncoated surface of the film along the c-axis direction. 6

1. INTRODUCTION

Research into the development of advanced RF sensors that employ superconducting circuitry is being carried out in the Cryogenic Exploitation of Radio Frequency (CERF) laboratory at Space an Naval Warfare Systems Center Pacific. The performance of these RF sensors are derived from the configuration of an array of highly sensitive magnetic field sensors known as Superconducting Quantum Interference Devices (SQUIDs). The characteristics of the SQUID circuit element is subsequently determined in part by the well-known physics of superconducting electronic tunnel junctions, referred to as Josephson junctions (JJs). Initial research into the performance and design of SQUID array RF sensors has involved the use of the low-temperature superconductor niobium, which becomes superconducting below a critical temperature of $T_c \approx 9$ K. Operating a niobium-based device then necessarily requires a large cryogenic cooling apparatus that can reach a temperature of T $\approx$ 4 K. A system-deployable sensor will require a significant reduction in size, weight, and power of the cryogenic packaging that in turn means operating at a much higher temperature close to T = 77 K. For this reason, a transition to research and development of SQUID arrays fabricated from the superconducting material $YBa_2Cu_3O_{7-\delta}$, (T_c = 92 K), is underway. In anticipation and support of this new direction of development a research effort began in FY12 under SSC Pacific Naval Innovative Science and Engineering (NISE) Basic and Applied Research (BAR) Program, wherein fundamental properties of the compound $YBa_2Cu_3O_x$ ($6 \leq$ x ≤ 7) were investigated along with the exploration of new combinations of multilayer hetero-structures composed of $YBa_2Cu_3O_x$ and multiferroic materials.

The evolution of the physical properties of high critical temperature (high-T_c) superconducting (HTS) cuprates across the charge doping $-$ temperature, $p - T$, phase diagram have been extensively studied for nearly three decades. An accurate understanding of this 'map' is essential to both the task of determining the mechanism of superconductivty in these materials and in developing technological applications. In many of the HTS compounds, the oxygen content controls the level of charge carrier (hole/electron) doping, which in turn determines the various possible electronic ground states, including the temperature T_c at which the material becomes superconducting. In the case of $YBa_2Cu_3O_x$, ($6 \leq x \leq 7$), the structure is such that oxygen content varies within the Cu-O chains, which are aligned along the b-axis of the lattice. The level of oxygen within the Cu-O chains subsequently, via a charge transfer process, determines the level of hole-doping in the CuO_2 planes where superconductivity, i.e., the pairing of electrons takes place.

Under the SSC Pacific NISE/BAR project, "Cryogenic Quantum RF Detection," we have been investigating the use of multiferroic perovskite oxides as the barrier material in HTS Josephson junctions in order to develop a junction with tunneling properties that are tunable via the complex functionality of the multiferroic barrier [1]. In addition, we have also recently established a new method by which to systematically investigate the physical properties of the $YBa_2Cu_3O_x$ system as a function of oxygen content wherein a fully oxygenated $YBa_2Cu_3O_7$ film is annealed in a low-pressure pure oxygen atmosphere while a steady-state thermal gradient is applied across the length of the film, resulting in a $YBa_2Cu_3O_{\nabla x}$ film [2–4]. It was shown that a film prepared in this manner has a monotonically varying oxygen content along the direction in which the applied thermal gradient was applied. However, rather than a smooth evolution of oxygen content along the entire sample length, three physically distinct regimes of oxygen distribution are observed such that, above $x \approx 6.89$ and below $x \approx 6.72$ the oxygen distribution smoothly varies along the sample length, but a discontinuity in oxygen content arises due to a large central region of the film stabilizing with an oxygen content of $x \approx 6.81$. No oxygenation states exist in the interval $x \approx$ [6.72 - 6.89] except for $x \approx 6.81$. The values of oxygen content, $x = 6.72$, 6.81, and 6.89, correspond to CuO_2 hole doping values of $p \approx$ 1/8, 1/7, and 1/6, respectively. The $p =$ 1/6 state lies close to the optimal doping value where the highest value of T_c is obtained. The $p =$ 1/8 and 1/7 doping values correspond to well-ordered Cu-O chain configurations wherein the oxygen sites within individual Cu-O chains are completely

occupied or completely empty [5–7]. The repeating patterns of full and empty chains form throughout the entire lattice. At oxygen levels where fully ordered chains are not possible, the oxygen in the chains tends to order in randomly distributed chain fragments which are superpositions of the fully ordered chain states [5–7].

Recently Wu et al. [8] demonstrated that HTS Josephson junctions can reliably be fabricated by focused ion beam (FIB) milling on an optimally doped $YBa_2Cu_3O_{7-\delta}$ film ($7-\delta \approx 6.91$). A gold over layer is deposited with a thickness just less than the depth to which the impacting gallium ions can penetrate. This limits the depth to which the gallium ions can mill away material from the $YBa_2Cu_3O_{7-\delta}$ film. Some gallium ions penetrate beyond the milled region into the $YBa_2Cu_3O_{7-\delta}$ film, causing low-energy ion damage to the lattice. The characteristics of the junction barrier are determined by controlling the thickness of the ion damaged link region. Such an approach represents a viable method for multilayer HTS circuitry. Currently, HTS circuitry is limited to single-layer fabrication designs. Having a multi-layer method available opens up the realization of more complex and physically dense circuitry. We investigate here whether the oxygen content within the lattice has an effect on the characteristics of the ion milling process. Having a large quantity of densely packed Josephson junctions on a $YBa_2Cu_3O_{\bigtriangledown x}$ film to precisely map out electronic structure and transport properties is a goal of our project. If we are to make use of the direct ion milling method of [8] to produce the desired array of Josephson junctions along the oxygen gradient, then we need to understand and control the milling process to produce uniform junctions. We find preliminary evidence here that oxygen ordering within the $YBa_2Cu_3O_{7-\delta}$ lattice significantly impacts the depth and profile of trenches produced by the ion milling process. Measurements examined here are limited to the underdoped region with $p \lesssim 1/8$ ($x \approx$ 6.69 - 6.71).

2. EXPERIMENT

A uniform $YBa_2Cu_3O_x$ film with a thickness of $t \approx 1500$ nm was grown on a <001> $SrTiO_3$ substrate ($\ell \times w$ = 1.0 cm $\times$ 1.0 cm) via the pulsed laser ablation method using a 248-nm laser. Following the method of [9], the target material used for the ablation process was prepared from stoichiometric quantities of Y_2O_3, $Ba(NO_3)_2$, and CuI. The film was deposited at 755 °C in 115 mTorr of flowing oxygen with the incoming gas directed into the laser plume directly above the substrate/film. Immediately following the film growth process, the oxygen pressure in the chamber was increased to 950 Torr at a rate of $\approx$ 100 Torr/min. The oxygen was flowed into the chamber through an alternate inlet such that the gas was not flowing across the sample. Concurrent with the increase in chamber pressure, the film was cooled to 450 °C at a rate of 10 °C/min and annealed at $\approx$ 950 Torr for a period of 12 hours. The sample is finally cooled to room temperature in a fully oxygenated $x = 7.0$ state at rate of 5 °C/min. The oxygen pressure at this temperature was 860 Torr. From this uniformly doped $YBa_2Cu_3O_7$ film, a $YBa_2Cu_3O_{\nabla x}$ film was prepared using the apparatus and method described in [4], with the only difference being that the film prepared and examined here was annealed in a slightly higher oxygen atmosphere with $P_{O_2} = 120$ mTorr. The annealing apparatus applies heat to one edge of the substrate/film with the opposite edge of the substrate/film in contact thermally sunk $-$ resulting in a linear thermal gradient across the sample ranging from 395 °C to 290 °C.

The film was directly etched using a FEI™ Nova 200 Nanolab™ DualBeam™ focused ion beam (FIB) without a gold film over layer. The beam is a gallium source and was run at an accelerating voltage of 30 kilovolts and a current of 0.5 nA. The FIB was configured such that each line was nominally patterned to be 14.25 μm $\times$ 2 μm using a serpentine pattern. (The beam spot is estimated as 20 to 50 nm in diameter). Each line was etched 6 min and 41 sec under the same conditions. A set of 16 parallel trenches were milled along the sample length such that the first trench is located at the low oxygen end of the sample and the last is located near the fully oxygenated end. A likely detwining of the film during the annealing process results in an alignment such that the a-axis (b-axis) runs parallel (perpendicular to the oxygen gradient [4]. Hence, the length of the trenches runs parallel to the b-axis of the film which, as mentioned above, is the same direction as the Cu-O chains. Three-dimension profiles of the ion milled trenches were obtained from Atomic Force Microscopy (AFM) measurements using an AIST-NT SmartSPM™ 1000.

X-ray diffraction measurements were taken in a Bruker D8 DISCOVER™ with a focused beam spot of $d \approx 350\mu$m 2D detector. The measurements were taken at spacings corresponding to the positions of the ion milled trenches along the direction of the applied thermal gradient so as to infer the local oxygen content via the value of the 2θ positions of the <00 ℓ> reflections. From the <00 10> and the <00 11> peak locations, the c-axis lattice parameter along the film sample length was determined and subsequently the hole doping level p of the film was inferred from equation (2) of [10]. Full details of the method of determining the c-axis length from the x-ray data are provided in [4]. From the extracted values of the c-axis length, calculated values of p are determined in the regions adjacent to the ion milled trenches. The values of p obtained are indicated in the legend of Figure 1(a) along with the corresponding trench profile obtained from AFM measurements.

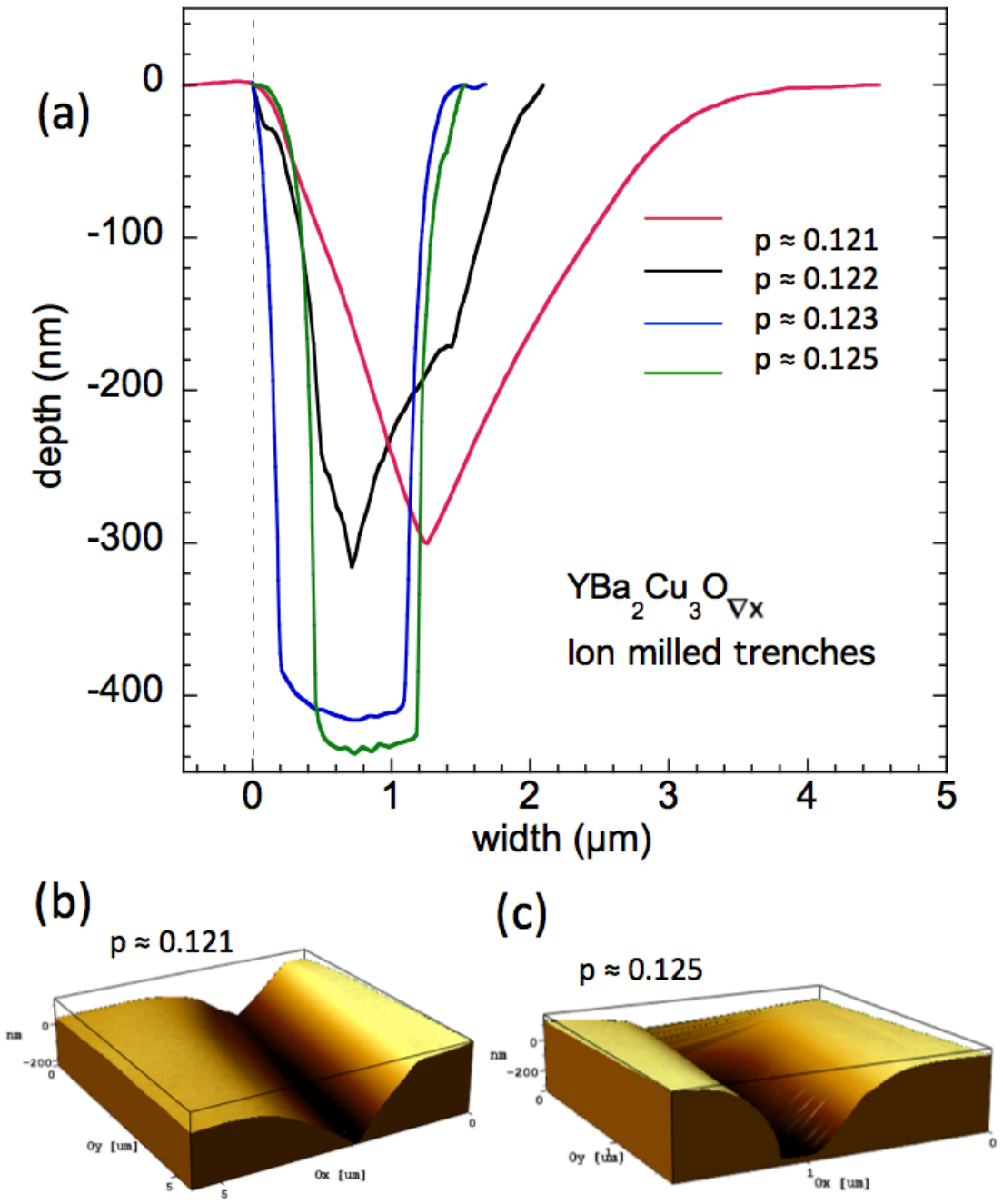

Figure 1. (a) 2-D profile taken from a section of the 3-D AFM images of ion milled trenches taken at locations having the CuO_2 plane doping values indicated. An upper limit on the error of the p values is estimated as Δp = 0.002. (b) 3-D AFM image of the ion milled trench taken at $p \approx 0.121$. (c) 3-D AFM image of the ion milled trenche taken at $p \approx 0.125$.

3. RESULTS & ANALYSIS

Results obtained from AFM imaging of the ion milled trenches examined here are shown in Figure 1. A clear evolution of the profile and depth of the trenches as a function of p (and corresponding oxygen content [1]) can be seen in the two-dimensional (2-D) plots taken from the larger sets of three-dimensional (3-D) AFM imaging. Three-dimensional images of the first and last trenches are shown in Figure 1 (b) and (c). The wedge shaped profile of the $p \approx 0.121$ trench is very similar to that obtained by [8] on an optimally doped ($p \approx 0.167$) film. The next trench, with $p \approx 0.122$, also exhibits a wedge shape and a nearly identical depth ($\approx$ 300 nm), however, the width of the trench has been reduced by $\approx$ 1/3. (The irregularity of the wedge shape is attributed to a local variation within the length of the trench). A definite change is observed in both the depth and shape of the trench for the subsequent lines at $p \approx 0.123$ and $p \approx 0.125$. The depth of both trenches has increased by 1/3 to $\approx$ 400 nm. More significantly though, the trenches have narrowed considerably, developed very steep walls, and have a nearly flat bottom, i.e., have transformed into a nearly rectangular profile. The observed trench profiles are consistent with a change in the "hardness" (a weakening of lattice bonds) and anisotropy of the material with respect to the impacting gallium ions. Having at this time a limited number of measurements to examine, the analysis and conclusions here are considered preliminary.

We can begin to make sense of our results by considering the evolving structure of the lattice being subjected to the ion milling process. Shown in Figure 2 (a) is the lattice structure of a fully oxygenated ($x = 7$) sample. Understanding the interrelationship of oxygen content, structural ordering, and charge doping of the CuO_2 plane is an important step in understanding the results from the ion milling profiles above. Oxygen diffuses most readily along the b-axis (the direction of the Cu-O chains, with the a-axis and c-axis diffusion rates approximately 10^2 and 10^6 times slower, respectively [11]. Charge carriers (holes) are transferred from the Cu-O chains to the CuO_2 planes via the apical O(4) oxygen. Evidence for the formation of electric dipole moments (aligned primarily along the c-axis) in the CuO_2 plane arising from this process has been put forth [12, 13]. From extensive analysis of comprehensive sets of x-ray diffraction measurements, a correlation of static displacements between apical O(2) oxygen and planar copper atoms two unit cells apart has been observed [14]. Within the oxygen ordering model for $YBa_2Cu_3O_x$ of [5–7] the highly correlated nature of electronic charge doping in the CuO_2 plane and oxygen ordering in the Cu-O chains has been examined. From the above observations (and others), the highly correlated structural and electronic nature of the $YBa_2Cu_3O_{7-\delta}$ system is well established.

Within [5–7], ordering within the Cu-O chain layer is described through a branching algorithm wherein the Ortho I (c = 0.5, $x = 7.0$) and Ortho II (c = 0.25, $x = 6.5$), (x = 2c + 6), structures are the generating structures for lower levels of stabilized oxygen ordering structures. The notation <1> and <10> denote the Ortho I and Ortho II chain states where a one or zero indicates a completely full or empty Cu-O chain, respectively, and an exponent denotes a repeated structure. The Ortho III structure, <110>, is formed from the combination of the Ortho I and II structures, i.e., <1> + <10> $\rightarrow$ <110>. From a comparison of the hole doping vs. oxygen content, p vs. 6 + x, data given in figure 4(a) of [10] to the branching algorithm dependence on the parameter c, we can infer that the $<1^40>$ fully ordered chain state (c = 0.40, $x = 6.8$) corresponds to the $p \approx$ 1/7 doping state, and the $<1^30110>$ (c = 0.36, $x = 6.72$) chain state corresponds very closely to the $p =$ 1/8 doping state ($p \approx 1/8 + \delta$, $\delta \approx 0.005$). The oxygen ordering structures within the plane containing the Cu-O chains is depicted in Figure 2(b) for the fully ordered Ortho I <1> and $p \approx$ 1/8 $<1^30110>$ states, and a disordered $p \lesssim 1/8$ state. Recall that the orientation of the trenches is parallel to the b-axis, i.e., the length of the trench runs along the direction of the Cu-O chains. As seen in Figure 2(b), the fully ordered oxygen structure of the $p \approx$ 1/8 state contains completely vacant

[1] The data in Figure 4a of Reference [10] were fit to the equation: 6 + x = 6.2623 - 1.601p + 63.409p^2 - 182.59p^3 over the range $6.25 < 6 + x < 7$.

Cu-O chains, resulting in natural anisotropic and relatively weak bonding seams in the lattice aligned along the b-axis. This highly ordered structure also likely serves as a natural lateral barrier to dispersion of the impacting Ga^+ ions and to the removal of atoms from the lattice by the ion milling process as depicted in Figure 2(c). In contrast, within the adjacent $p \lesssim 1/8$ region the oxygen distribution, and hence the lattice bonds, are disordered and thus isotropically distributed, both within the plane containing the Cu-O chains, and along the c-axis, i.e., there is no correlation of oxygen order between vertically adjacent Cu-O chains.

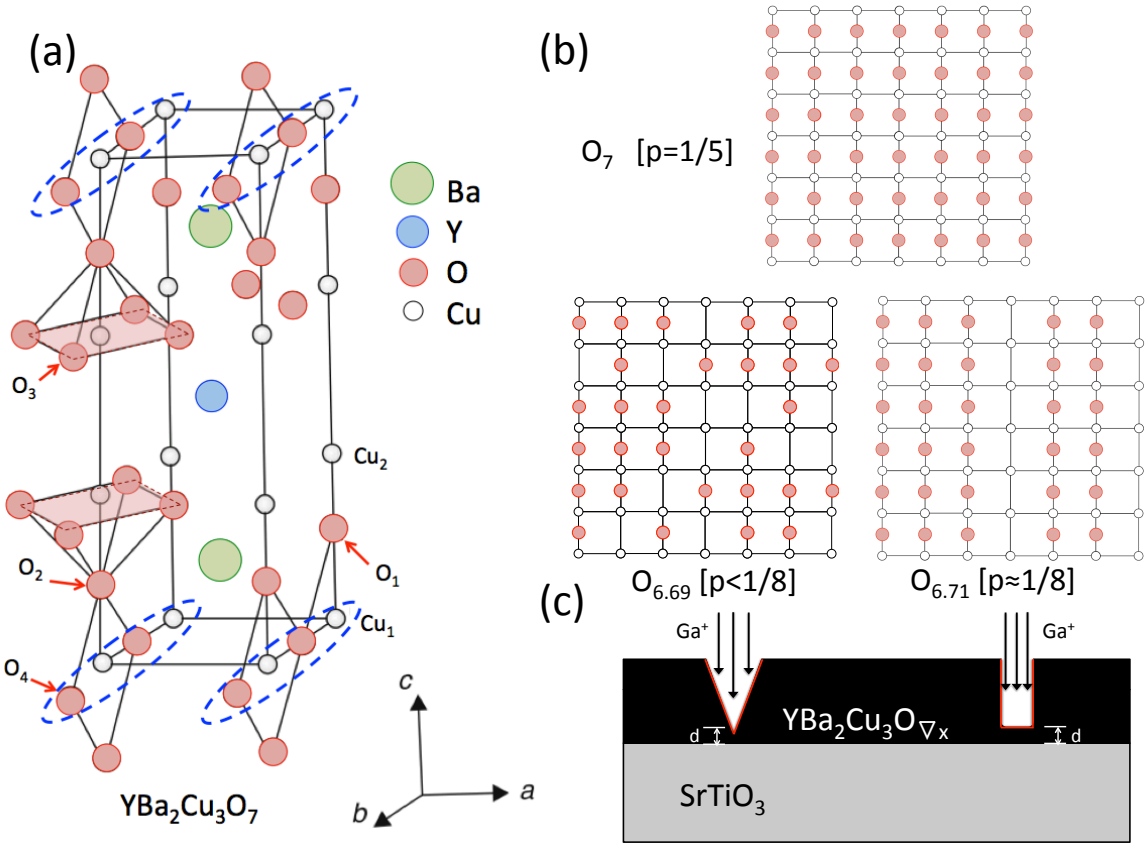

Figure 2. (a) Lattice structure of fully oxygenated $YBa_2Cu_3O_7$. Cu-O chains are highlighted with blue dashed ovals. The superconducting CuO_2 planes are highlighted with red dashed panels. For clarity, not all oxygen atoms are shown in the CuO_2 plane. (b) Oxygen ordering in the plane containing the Cu-O chains. Depicted are the well-ordered chain states with $x = 7.0$ ($p \approx 0.20$) and $1/8^{th}$ doping ($x \approx 6.71$) states, as well as the disordered (broken chain) state with $p \lesssim 1/8$. (c) Depiction of the direct ion milling process used to fabricate Josephson junctions in $YBa_2Cu_3O_{7-\delta}$ along with the resulting trench profile in the two regions having doping values indicated in panel (b) above. As described in the main text, Ga^+ ions impact the uncoated surface of the film along the c-axis direction.

4. CONCLUSION

We have examined the impact of oxygen stoichiometry in $YBa_2Cu_3O_x$ on the depth and profile of directly ion milled trenches in the mid under-doped region having oxygen content $x \approx$ [6.6 - 6.7] ($p \approx$ [0.121 - 0.125]). We have found preliminary evidence for a correlation of oxygen content on the resulting profile of the ion milled trench. With respect to our initial purpose of investigation, these results indicate that if we are to produce Josephson junctions at known positions on a $YBa_2Cu_3O_{\nabla x}$ film via the direct ion milling process, it is necessary to either alter the milling conditions to compensate for the effects of the local oxygen content on junction geometry, or to account for these differences when analyzing junction properties in different regions. Furthermore, it appears likely that the oxygen distribution of fully ordered $p \approx$ 1/8 Cu-O chain state impacts the ion milling process by providing a natural grating (lateral barrier) to impacting ions. If such an analysis is accurate, then we will expect to see a similar result for the trenches located in the region having having an oxygen content corresponding to the $p \approx 1/7$ state ($x \approx$ 6.81). If this effect can be well established and controlled, it then opens up the possibility to exploit this for the Navy's benefit. Such a profile would naturally result in smaller area needed to produce a Josephson junction by the direct ion milling process. In particular, samples can be prepared with $p = 1/8$ (or $p = 1/7$), ion milling can be carried out to obtain the desired narrow and flat trench profile, and then the film can be re-oxygenated (re-annealed) to the desired doping state (or profile). Using this process would potentially result in a low cost method for producing devices having a higher density of Josephson junctions than by direct ion milling of an optimally doped film. Use of a gold over layer in the milling process will result in a narrowing of the milled section down to the order of 20 nm - 50 nm, as demonstrated in [8]. Combined with the apparent ion beam confining effects of the well ordered Cu-O chain states ($p = 1/8$), arrays of Josephson junctions a few tens of coherence lengths apart ($\xi \sim 10$ Å) could be fabricated resulting in a density approaching 10^8/cm^2. [2]

.

[2] We have estimated junction density using a junction barrier width of 20 nm, a lateral junction length of 10 μm, a spacing between junctions in a linear array as 30 nm, and spacing between arrays as 10 μm. Junction density = 1/(50 nm $\times$ 20 μm) = 10^8/cm^2.

REFERENCES

1. B. J. Taylor. 2014. "Electronic Circuitry Having Superconducting Tunnel Junctions with Functional Electromagentic-Responsive Tunneling Regions." (Patent Pending). NC# 102229.

2. B. J. Taylor. 2013. "System and Method for Producing a Sample Having a Monotonic Doping Gradient of a Diffusive Constituent or Interstitial Atom or Molecule." (Patent Pending). NC# 102010.

3. B. J. Taylor. 2014. "Apparatus and Methods for Production of Mono-Crystalline, c-axis Oriented, Epitaxial $YBa_2Cu_3O_{7-\delta}$ Films." NC# 103086.

4. B. J. Taylor, C. A. McElroy, I. K. Lum, A. M. Leese de Escobar, M. C. de Andrade, T. J. Wong, E. Y. Cho, and M. B. Maple. In print. "Correlation of Structural, Magnetic, and Electronic Transitions of a 'Charge Gradient' $YBa_2Cu_3O_{\nabla x}$ Film."

5. D. de Fontaine, G. Cedar, and M. Asta. 1990. "Low-Temperature Long-Range Oxygen Order in $YBa_2Cu_3O_z$," *Nature 343*:544 – 546.

6. R. McCormack and D. de Fontaine. 1992. "Oxygen Configurations and Their Effect on Charge Transfer in Off-Stoichiometric $YBa_2Cu_3O_z$," *Physical Review B 45*:12976.

7. D. de Fontaine, V. Ozolins, Z. Islam, and S. C. Moss. 2005. "Origin of Modulated Structures in $YBa_2Cu_3O_{6.63}$: A First-Principles Approach," *Physical Review B 71*:212504.

8. C. H. Wu, F. J. Jhan, J. H. Chen, and J. T. Jeng. 2013. "High-T_c Josephson Junctions Fabricated by Focused Ion Beam Direct Milling. *Superconductor Science and Technology*," *26*:025010.

9. X. G. Zheng, M. Suzuki, C. Xu, H. Kuriyaki, and K. Hirakawa. 1996. "Synthesis of Ca-Substituted $Y_{1-x}Ca_xBa_2Cu_4O_8$ at Ambient Pressure Using CuI," *Physica C 271*:272 – 276.

10. R. Liang, D. A. Bonn, and W. N. Hardy. 2006. "Evaluation of CuO_2 Plane Hole Doping in $YBa_2Cu_3O_{6+x}$ Single Crystals," *Physical Review B 73*:8505(R).

11. S. J. Rothman, J. L. Routbort, U. Welp, and J. E. Baker. 1991. "Anisotropy of Oxygen Tracer Diffusion in Single-Crystal $YBa_2Cu_3O_{7-\delta}$," *Physical Review B 44*:2326.

12. N. Chandrasekhar, O. T. Valls, and A. M. Goldman. 1994. "Charging Effects Observed in $YBa_2Cu_3O_{7-x}$ Films: Influence of Oxygen Ordering," *Physical Review B 49*:6220.

13. G. Grigelionis, E. E. Tornau, and A. Rosengren. 1996. "Effect of an Electric Field on Oxygen Ordering and Superconducting Temperature of $YBa_2Cu_3O_{6+x}$ Thin Films," *Physical Review B 53*:425.

14. J. Etheridge. 1996. "Structural Perturbations at Intervals of the Coherence Length in $YBa_2Cu_3O_{7-\delta}$ ($\delta < 0.1$)," *Philosophical Magazine A 73*:643 – 668.

REPORT DOCUMENTATION PAGE

Form Approved
OMB No. 0704-01-0188

PLEASE DO NOT RETURN YOUR FORM TO THE ABOVE ADDRESS.

1. REPORT DATE *(DD-MM-YYYY)*	2. REPORT TYPE	3. DATES COVERED *(From - To)*
September 2014	Final	

4. TITLE AND SUBTITLE

Investigation of the Effects of Oxygen Content in $YBa_2Cu_3O_x$ on the Depth and Profile of Direct Ion Milled Trenches

5a. CONTRACT NUMBER

5b. GRANT NUMBER

5c. PROGRAM ELEMENT NUMBER

6. AUTHORS

Benjamin Taylor
Teresa Emery
Susan Berggren

5d. PROJECT NUMBER

5e. TASK NUMBER

5f. WORK UNIT NUMBER

7. PERFORMING ORGANIZATION NAME(S) AND ADDRESS(ES)

SSC Pacific, 53560 Hull Street, San Diego, CA 92152–5001

8. PERFORMING ORGANIZATION REPORT NUMBER

TR 2049

9. SPONSORING/MONITORING AGENCY NAME(S) AND ADDRESS(ES)

Naval Innovative Science and Engineering (NISE) Program (Applied Research
SSC Pacific, 53560 Hull Street, San Diego, CA 92152–5001

10. SPONSOR/MONITOR'S ACRONYM(S)

11. SPONSOR/MONITOR'S REPORT NUMBER(S)

12. DISTRIBUTION/AVAILABILITY STATEMENT

Approved for public release.

13. SUPPLEMENTARY NOTES

14. ABSTRACT

Research being carried out in the Cryogenic Exploitation of Radio Frequency (CERF) laboratory at Space and Naval Warfare Systems Center Pacific (SSC Pacific) into the development of advanced superconducting RF sensors known as Superconducting Quantum Interference Device (SQUID) arrays is transitioning from the development and study of devices fabricated from the low-temperature superconductor niobium to system-deployable devices made from the high-temperature superconductor $YBa_2Cu_3O_x$.

15. SUBJECT TERMS

Mission Area: Applied Research

radio-frequency sensors
superconducting quantum interface devices (SQUID)
Josephson junctions
high-temperature superconductor
ion milling process
$YBa_2Cu_3O_x$

16. SECURITY CLASSIFICATION OF:			17. LIMITATION OF ABSTRACT	18. NUMBER OF PAGES	19a. NAME OF RESPONSIBLE PERSON
a. REPORT	b. ABSTRACT	c. THIS PAGE			Benjamin Taylor
U	U	U	U	16	19B. TELEPHONE NUMBER *(Include area code)* (619) 553-4905

INITIAL DISTRIBUTION

84300	Library	(2)
85300	Archive/Stock	(1)
71730	B. Taylor	(1)
71730	T. Emery	(1)
71730	S. Berggren	(1)

Defense Technical Information Center
Fort Belvoir, VA 22060–6218 (1)

Approved for public release.

SSC Pacific
San Diego, CA 92152-5001